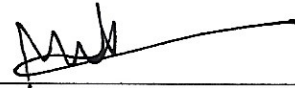# Extending the Bandwidth of a Cryogenic Far Infrared Photodetector for Nanospectroscopy

A thesis submitted in partial fulfillment of the requirement
for the degree of Bachelor of Science in
Physics from the College of William and Mary in Virginia,

by

Micheal E. Crotty

_____

Advisor: Prof. Mumtaz Qazilbash

_____

Senior Thesis Coordinator: Prof. Seth Aubin

Williamsburg, Virginia

May 2019

Contents

Acknowledgments

List of Figures

Abstract

This thesis covers the improvement of the circuit design for a cryogenic far-infrared photodetector for nanospectroscopy, specifically on increasing the bandwidth of the preamplifier circuit. Increasing the bandwidth of this preamplifier circuit will allow us to study currently-inaccessible properties of materials in the far infrared spectral range with nanometer scale spatial resolution. Studying materials in the far-infrared range gives us the ability to investigate phonons in the materials as well as electronic structure and dynamics.

After searching for non-idealities in the circuit such as parasitic capacitances, which can affect the bandwidth at higher frequencies, we look at changing the opamps and feedback resistors in order to give us a strong signal gain as well as a bandwidth of up to 1 MHz. We have found experimentally that, an OPA637 op amp and a 500 kΩ feedback resistor gives us the highest bandwidth at around 800 kHz, as well as the most consistent results.

Chapter 1

Introduction

Light plays a very important role in many different areas of physics, especially modern experimental physics. Light is an electromagnetic wave and diffraction-limited, which means that light cannot be accurately resolved to a point. The main objectives of the lab that I am working with are to study the properties of materials at resolutions that are smaller than the diffraction limit of light. The diffraction limit can be calculated using the equation,

$$d = \frac{\lambda}{2NA} \quad , \tag{1.1}$$

where λ is the wavelength of light and NA is the numerical aperture [1]. With a technique known as scattering-type scanning near-field optical microscopy (s-SNOM), we can use an atomic force microscope (AFM) and focus light on a tip which acts as an antenna to the light. The s-SNOM method, as shown in Fig 1.1, allows spatial resolution determined by the radius of curvature the AFM tip [2]. Specifically, we are studying the far-infrared wavelengths ($\leq 800\ cm^{-1}$) of light because materials have optical phonons which occur only in the far-infrared spectrum of light. These phonons can tell us about the lattice dynamics in the material. The detector that we want to use can reach wavelengths up to 30 microns in the far infrared. This detector takes in light that has been scattered by the AFM tip and converts the light into a current through the photoconductor which passes through the preamp circuit within

the detector module. Unfortunately, this new detector is not fast enough (reading only up to 30 kHz) to observe the higher harmonics of the AFM tip modulation which occur up to 1MHz.
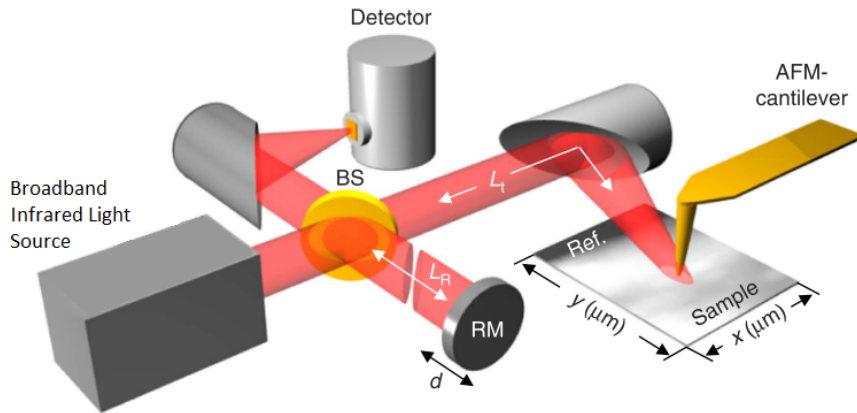
Figure 1.1: s-SNOM Diagram. This is a diagram depicting the s-SNOM method showing the light source, AFM tip, and the detector. (image adapted from 'Hyperspectral infrared nanoimaging of organic samples based on Fourier transform infrared nanospectroscopy' Nature Communications volume 8, Article number: 14402 (2017)

1.1 The Goal of the Experiment/Research

My main goal in this project is to improve the speed of the electronic circuit of the new detector, as seen in Fig 1.2, so that it can properly observe the higher harmonics of the modulation of the AFM tip. The AFM tip oscillates at 250 kHz, and we want to be able to detect up to the 4th harmonic (1 MHz) because these higher harmonics contain the near field signal and simultaneously reduce the background far-field signal.
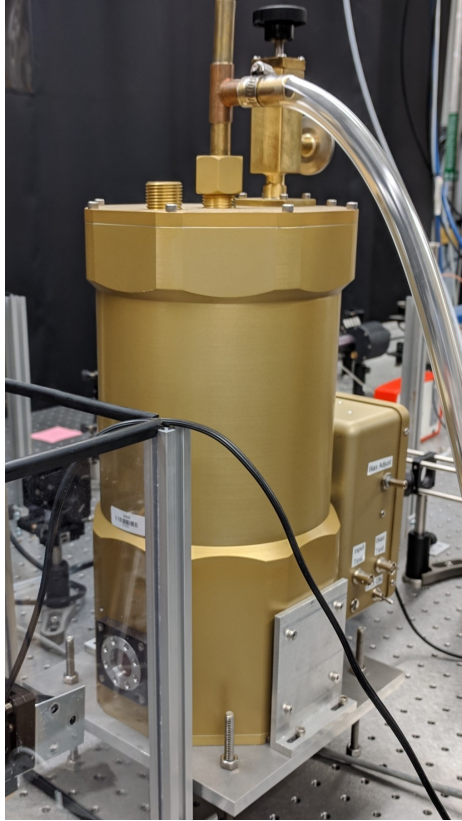
Figure 1.2: Detector. This is an image of the detector module we are working with. The circuit that I am studying lies within the detector module, inside the box that you can see attached to the back of the cryogenic vessel. The liquid helium cooled detector element is mounted inside the cryogenic vessel.

Inside the circuit box of the detector is a preamplifier circuit, which you can see modeled in LTspice in Fig. 1.3, that amplifies the input signal from the detector. This circuit consists of a first transimpedance stage, which converts the photocurrent signal to a voltage signal, and a second gain stage, which amplifies the gain of the voltage signal by a factor of 10. In the initial configuration of the circuit, the first stage uses an OPA111 operational amplifier (op amp) with a choice of either a 4.15 MΩ or 500 kΩ feedback resistor (Rfstage 1 in Fig. 1.3), and the second stage uses an OPA27 op amp. These three components are the main components that I can change to try and improve the bandwidth of this circuit. During normal operation of

the photodetector module, the 4.15 MΩ resistor is cooled down to 4.2 Kelvin along with the photodetector element (Rd in Fig. 1.3), whereas the 500 kΩ resistor is at room temperature. The cooling with liquid helium can reduce the Johnson noise in the circuit, which comes from thermal agitation in electronic components [3].
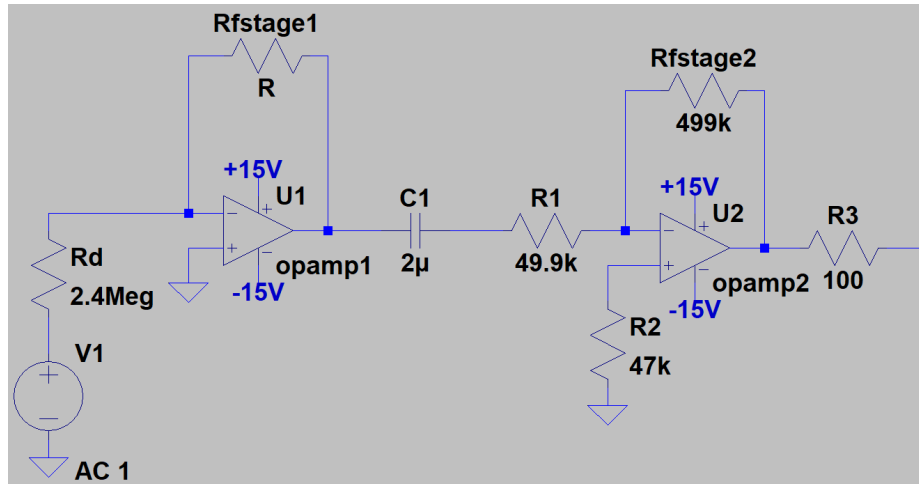
Figure 1.3: Preamp Circuit Diagram. This circuit model, built in LTspice, represents our preamplifier circuit. Objects of variance include Rfstage1, opamp1, and opamp2. We change the value of these components to improve the bandwidth of the circuit.

4

Chapter 2

Theory

In this project, I cover a variety of different topics within the field of electronics. It is important to understand these topics and the processes that we take in order to improve our preamplifier circuit.

2.1 Opamps

The basic idea of this project is to choose the best operational amplifier, better known as op amps, to give our circuit the highest bandwidth we can, preferably up to 1MHz. An op amp is an electronic component that takes either an input signal of current or voltage, and amplifies the input into a larger (or smaller) output current or voltage [4]. In our situation, input signal comes from a photoconductor which, according to Antoni Rogalski's book on infrared detectors [5], is a type of photodetector that can be modeled as a radiation sensitive resistor. Our photodetector element is boron-doped silicon, and the photodetector module was purchased from Infrared Laboratories. You can see this photoconductor modeled as the 2.4 MΩ resistor in Fig. 1.3.

2.2 Bode Plots and Gain

In this thesis, we show Bode plots that compare the gains of different configurations of the circuit to help us see what op amp and feedback resistor to choose to get us to

the highest possible bandwidth. To understand this, we must first understand what gain is. Gain is a simple term in op amp circuits that describes the amount by which the input signal has been amplified using the simple equation,

$$G_{linear} = \frac{R_{out}}{R_{in}} \quad , \tag{2.1}$$

where R_{out} is our feedback resistor, and R_{in} is our photoconductor's resistance. A Bode plot shows this gain calculated in decibels on the y-axis and the input frequency on a logarithmic scale on the x-axis. Gain in decibels can be calculated from the equation,

$$G_{decibels} = 20 * log_{10}(G_{linear}) \tag{2.2}$$

The bandwidth can be determined by looking at the -3 dB point on a Bode plot. This is the point at which the gain has decreased by 3 dB. The value of the feedback resistor is what controls the gain of the circuit. The feedback resistor that we will change in this circuit is seen in Fig. 1.3 as the resistor named $Rfstage1$.

2.3 Transimpedance Amplifiers

Because the signal is coming from a photodetector, we have an input current running into the input of our op amp. Since our circuit amplifies an input current into an output voltage, we have a transimpedance amplifier. Knowing that this is a transimpedance amplifier, we can choose op amps that work best in high speed transimpedance applications.

Chapter 3

Experimental Methods and Results

To begin this project, I was given some experimental data taken about a year ago from the preamplifier circuit board that is connected to the photodetector. The data was acquired by sending a signal source through the photodetector which gets sent through the preamp circuit. This data shows the voltage gain in decibels of the circuit as the frequency of the AC signal increases. I then compared this data to a simulation, as seen in Fig. 3.1, of the same circuit modeled in LTspice, a simulation software for modeling circuits. As you can see, the experimental data does not match up to the simulation. The bandwidth of the experimental data is only around 40 kHz, whereas the expected bandwidth from the simulation is around 250 kHz. This means that there must be some kinds of non-idealities that are not accounted for in the Spice simulation that are showing up in our experimental data.
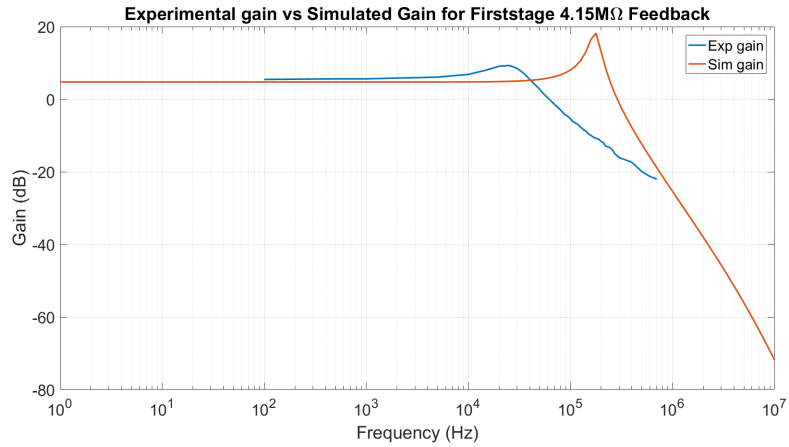
Figure 3.1: Experimental and Simulated OPA111 First Stage. This plot shows the difference in bandwidth in our experimental results for OPA111 in the first stage of the circuit with the 4.15 MΩ feedback resistor

3.1 Varying Parasitic Capacitances

According to J. A. Woody in a technical report [6], "All components and their leads exhibit parasitic, or stray, capacitances, inductances, and resistances". This means that each electronic component can have resistive, capacitive, and inductive properties, and can be modeled as shown in Fig. 3.2.
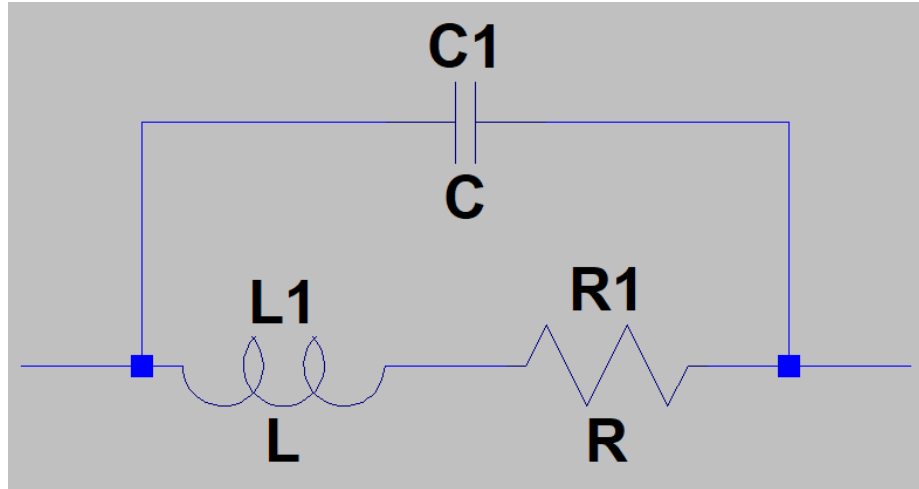
Figure 3.2: Resistive, Capacitive, and Inductive properties. This diagram shows the ways that an eletrical component such as a resistor, capacitor, or inductor can have all three resistive, capacitive and inductive properties.

The data sheets we were given on the components in the circuit only listed the parasitic capacitance of the 4.15 MΩ feedback resistor, which told us that the value of the parasitic capacitance for this component could be anywhere from 0.002 pF to 0.5 pF. Because of our lack of data from these components, I made some plots that show variance in parasitic capacitance to understand how a capacitance on any particular component may affect the gain of our circuit. You can see in Fig. 3.3 that I add capacitors in parallel across the feedback resistor and the detector element, to model parasitic capacitance in these two elements. I also added a capacitor connecting from the inverting input of the op amp to ground to model stray capacitance that may come from the long (about 30 cm) bundle of wires connecting the circuit board itself to the detector. It is important to note that parasitic inductances will also occur, and may affect the components, such as the feedback resistors and wires within the circuit. I used an equation from Inductance calculations [8],

$$M = 0.002l[ln\left(\frac{2l}{d}\right) - 1 + \frac{d}{l} + \frac{1}{4}\frac{d^2}{l^2}] \qquad (3.1)$$

to calculate the mutual inductance between two parallel wires, where l is the length of the wire in cm and d is the distance between the wires. This is the case for our 30 cm long bundle of 6 wires, 3 of which are powered, so, calculating the inductance between two wires turns out to be about 440 nH, and if there are 3 parallel inductances, this totals to around 147 nH. This inductance is very small and makes negligible changes to our data at 1 MHz.
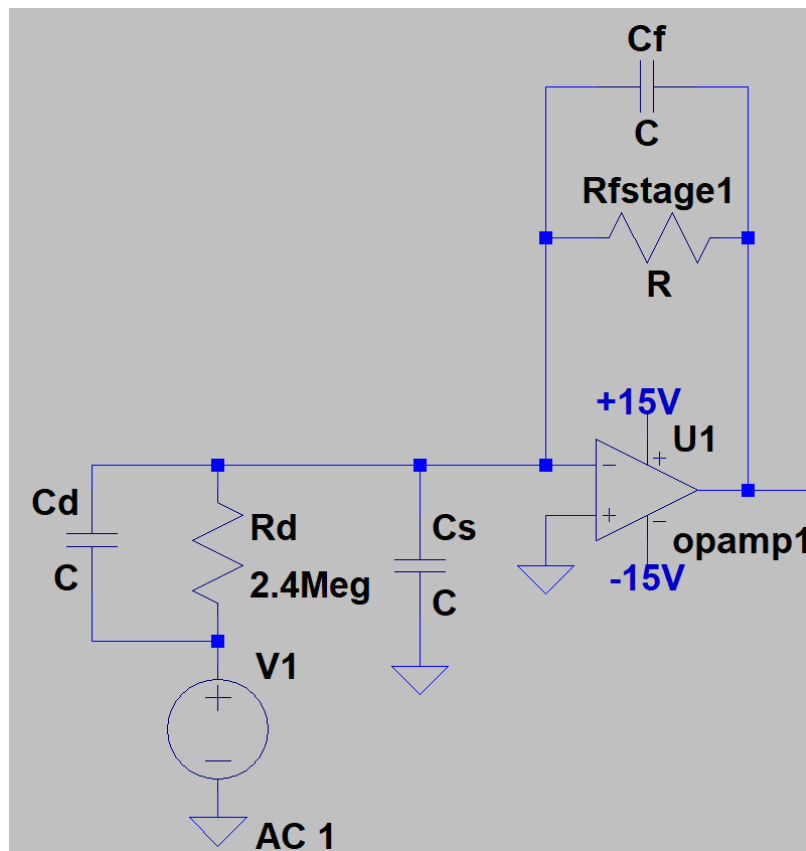
Figure 3.3: Circuit First Stage with Parasitic Capacitance. This is only the first stage of out circuit, now with some capacitors added to model parasitic capacitances. Cd is the capacitance from the detector element, Cs is the stray capacitance from wires, and Cf is the capacitance from our feedback resistor.

First, I vary the parasitic capacitor across the feedback resistor, which in this case is the 4.15 MΩ resistor. From Fig. 3.4, the added capacitor does not seem to affect the

overall bandwidth of the circuit too much, but rather smooths out the spike in gain. This spike in gain happens because a singularity occurs in the gain at the frequency where the feedback capacitance takes over the feedback resistance as the dominating factor for gain. Since the feedback capacitance is zero originally, the spike is large, and as we increase the capacitance, the spike will shrink. I used the values 0 pF-0.5 pF because that is what was given in the specifications for this particular component on the circuit board.
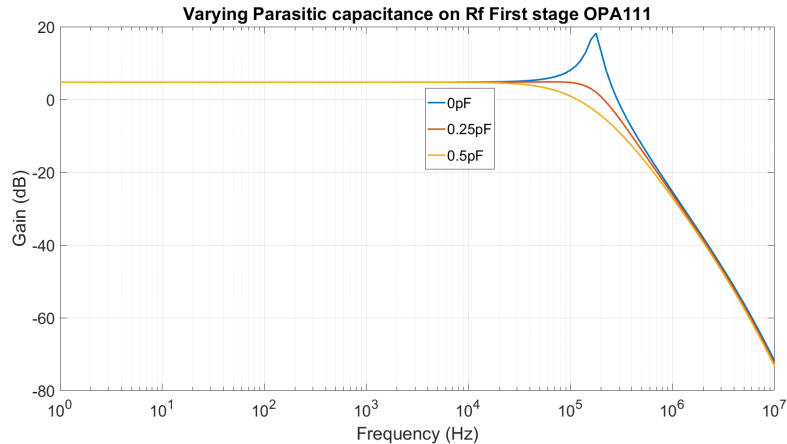
Figure 3.4: Varying Parasitic Capacitance on Rf. Here we vary the parasitic capacitance on the feedback resistor. We use the feedback resistor of value 4.15 MΩ for this simulation.

Next, I look at how varying the value of the stray capacitor affects the simulated gain of the circuit. This stray capacitance shows up between the wire to the inverting input of the op amp and ground. In Fig. 3.5, it is fairly easy to see that the bandwidth of the circuit seems to decrease as we increase the value of the stray capacitor. The values of 0-80 pF were chosen because these are typical values of capacitance that can be found between wires. We actually found the capacitance between these wires later with an equation from Jackson [7],

$$C = \frac{2\pi\epsilon}{\cosh^{-1}\left(\frac{d^2-2a^2}{2a^2}\right)} \quad , \tag{3.2}$$

where ϵ is the permittivity of the insulation of the wire, d is the center to center distance between the two wires and a is the radius of the wire. This will calculate the capacitance in pF/m between the active wire connecting to the input terminal of the op amp and a grounded wire. Knowing these values from the specifications of the wires from the data sheet of our circuit, we found the capacitance between two wires in the bundle to be about 30 pF/ft. Since there are three grounded wires in the bundle, and these wires can be modelled in parallel to each other, we find the total stray capacitance from these wires to be about 90 pF, which is why we choose this value for the stray capacitance when modeling all the capacitances together later.

Figure 3.5: Varying Stray Capacitance in Wires. Here we vary the value of the stray capacitance that occurs in the wires.

Lastly, I vary the parasitic capacitance across the detector element, which is modeled as a resistor, so I can model a capacitor in parallel similar to what I did for the feedback resistor. In Fig. 3.6, the slope of the gain roll off changes by decreasing as the value of the capacitor increases.
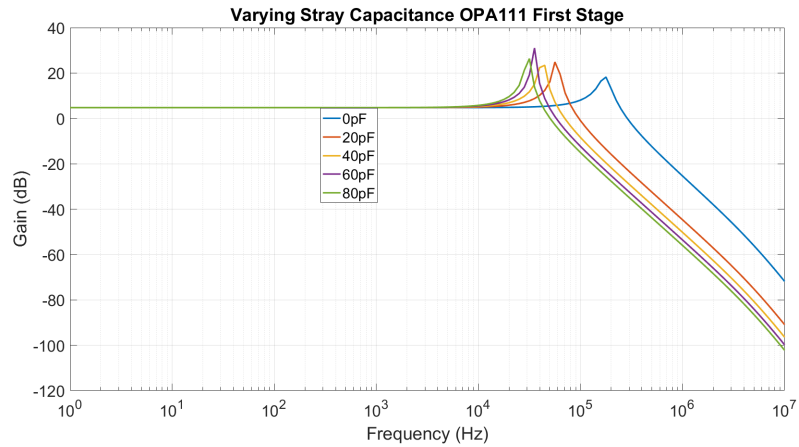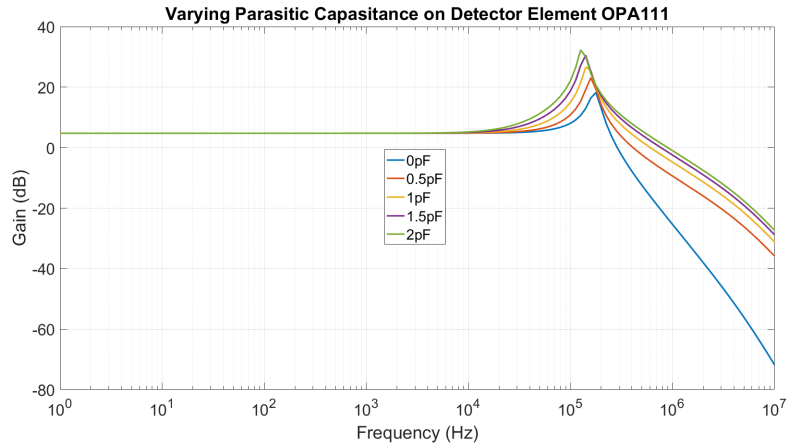
Figure 3.6: Varying Parasitic Capacitance on Photoconductor. Here we vary the value of the parasitic capacitance on the detector element.

Choosing values of capacitance that most closely match our experimental data, as well as stay inside the ranges of parasitic capacitance known from the component data sheets, I plotted a simulation of the first stage of our circuit with most of the non-idealities factored in. We have a parasitic capacitance of 0.5 pF across the 4.15 MΩ feedback resistor, 90 pF of stray capacitance from the wires bundled together as well as their capacitances connecting to the input terminals, and 2 pF of parasitic capacitance across the detector element. It is seen in Fig. 3.7 that this very closely resembles the experimental data, which means that these parasitic capacitances have been nearly all modeled.
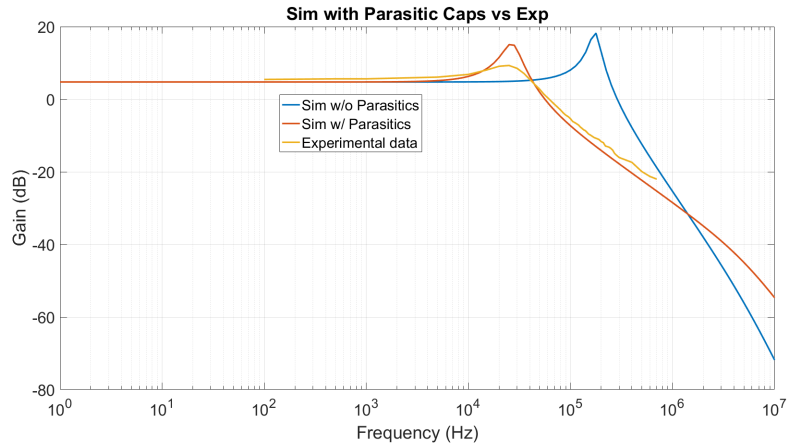
Figure 3.7: Circuit with all Parasitic Capacitances. In this plot, we include reasonable values for all the types of parasitic capacitances that may be found in our circuit and we compare it to the experimental data for the same circuit.

3.2 Choosing other Op amps

Now we need to look at new op amps that may perform better, in terms of bandwidth, for our circuit so that we can eventually replace the OPA111 and OPA27 to increase the bandwidth of the preamp circuit. For this we chose op amps such as the OPA637 and THS4631 with specifications seen in Fig 3.8. We chose the OPA637 and THS4631 because they are high speed op amps, which mean that they are supposed to operate with a bandwidth of higher frequencies. In combination with their high speed, these op amps are also recommended for use in transimpedance applications, which makes them ideal for a situation such as ours. The gain bandwidth product (GBW) of the OPA637 as well as the THS4631 are both higher than the initial GBW of the OPA111. The higher GBW suggests that these op amps should theoretically give a higher bandwidth than the OPA111 in our circuit.

Op Amp	Noise Spec.	Gain Bandwidth Product	Supply V	Input Impedance
OPA111	$8nV/\sqrt{Hz}$ at 10kHz	2MHz	±15V DC typ	10^13 Ω
OPA637	$4.5nV/\sqrt{Hz}$ at 10kHz	80MHz	±15 V DC typ	10^13 Ω
OPA27	$4.5nV/\sqrt{Hz}$ AT 1kHz	8MHz	±22 V DC max	2x10^9 Ω
THS4631	$7nV/\sqrt{Hz}$	210MHz	±15 V DC typ	10^9Ω

Figure 3.8: Op amp Specification Table. This shows the noise, GBW, input impedance, and supply voltage recommendations for the different op amps we used in our experiments.

Looking at Fig. 3.9, we can see that the OPA637 gives us a simulated bandwidth of about 700 kHz and the THS4631 gives us a simulated bandwidth of about 2.5 MHz with the 4.15 MΩ resistor in the first stage compared to the 250 kHz simulated bandwidth that the OPA111 gives. Same goes for the 500 kΩ resistor in the first stage for both the OPA637 and THS4631 having simulated bandwidths of 1.9 MHz and 7 MHz respectively compared to 750 kHz OPA111.
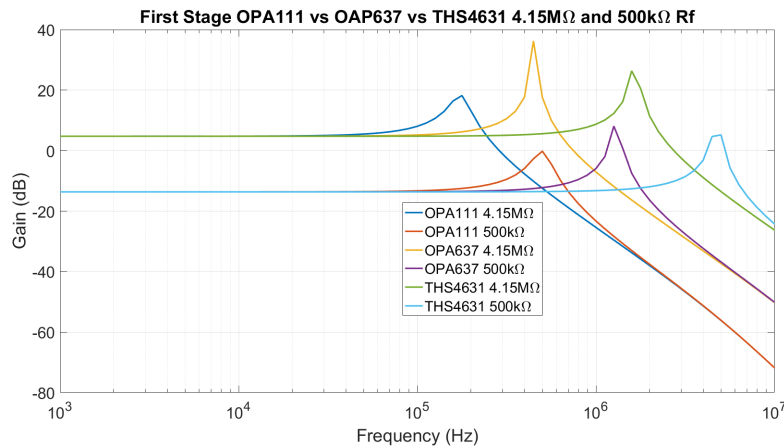

Figure 3.9: Simulated OPA111-OPA27, OPA637-OPA637, THS4631-THS4631 First and Second Stage. This is a simulation of our circuit for the first and second stage with the OPA111-OPA27 op amps, as well as the new OPA637 and THS4631 op amps.

3.3 Breadboard Simulation

At this point, we decided that we needed to test out these other op amps in a real circuit to compare them to the old experimental data for the OPA111 circuit. The detector is very expensive to run because we need liquid helium to cool down some of the specific components, so the most simple, and cost-effective, way to test the components without using the preamp circuit in the detector is to construct a very similar circuit with similar components on a breadboard. To do this, we got components to match all of the components from the circuit board and build the circuit from scratch on a breadboard as seen in Fig. 3.10. Unfortunately, we were not able to get a hold of a 4.15 MΩ resistor or a 2.4 MΩ resistor, so we placed 2x 2 MΩ resistors and a 150 kΩ resistor in series for the 4.15 MΩ resistor, and a 2 MΩ and 400 kΩ resistor in series for the 2.4 MΩ resistor. I acknowledge that this may have caused some extra parasitics to occur, but this is as close as we can get to modeling the actual circuit on a breadboard. To reduce AC noise coming from the DC power supplies, we added some decoupling capacitors to the plus and minus Vcc terminals to the op amps, then took data for all three op amps in the first stage.
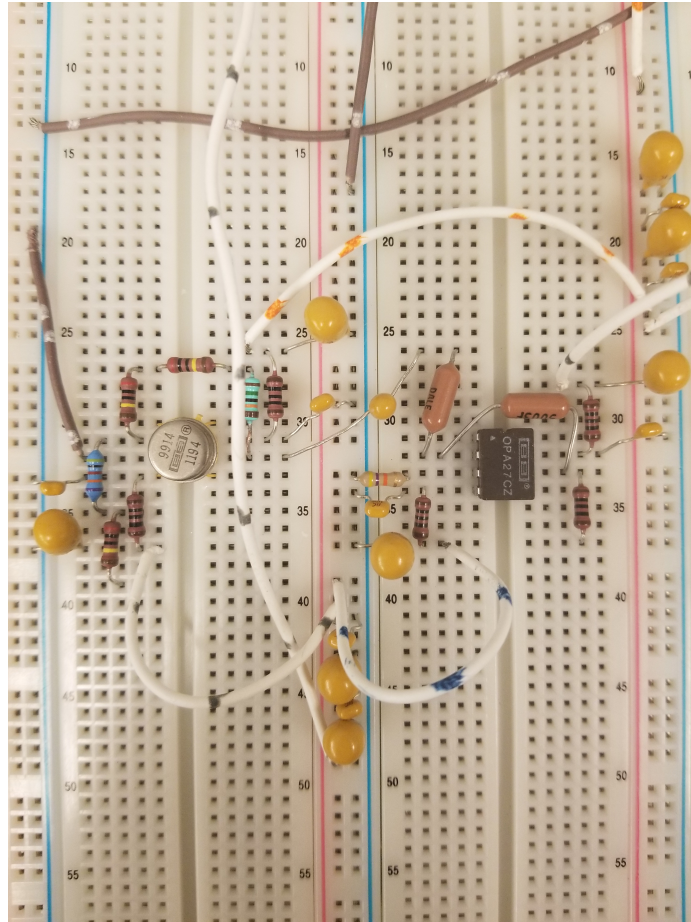
Figure 3.10: Breadboard Circuit. This is our breadboard circuit used for comparing the op amps in the original circuit under more 'realistic' conditions than just the LTspice simulations. The op amps in this image are the OPA111 and OP27 from our detector circuit board. We swapped them out for the OPA637 and THS4631 when we took data for those.

At first we ran into voltage oscillation and railing issues when we attempted to take data while the first and second stages were connected, so we were only able to take data for the first stage by itself; however, is still a good set of data to help us determine which op amp would work best for us. Later, we added a better decoupling for the power supply as well as cutting the leads of the components to be shorter, which improved the noise levels in our circuit somewhat. This also allowed us to be able to take data of both stages connected for the OPA111-OPA27 circuit for both

the 4.15 MΩ and the 500 kΩ feedback resistors as well as the OPA637-OPA637 and THS4631-THS4631 circuit for the 500 kΩ feedback resistor, but not for the 4.15 MΩ feedback resistor, but that will be discussed more later.

From Fig. 3.11, we notice that the breadboard simulation of our circuit with the 4.15 MΩ feedback resistor and OPA111 actually very closely resembles the exper-imental data for the 4.15 MΩ feedback resistor circuit on the circuit board. This confirms that our breadboard simulation for the first stage of the preamp circuit is accurately representing the real circuit.

Figure 3.11: Breadboard OPA111 4.15 MΩ. This plot shows gain for the first stage with the 4.15 MΩ feedback resistor of the breadboard simulation compared with the experimental data for the actual circuit as well as the spice simulation for the circuit.

Swapping out the 4.15 MΩ feedback resistor for the 500 kΩ resistor in our bread-board circuit, we see from Fig. 3.12 that the gain has a slight dip down with almost no peak before falling off at around 200 kHz. This is an interesting feature that we keep note of later with the other breadboard simulations with the 500 kΩ feedback resistor.
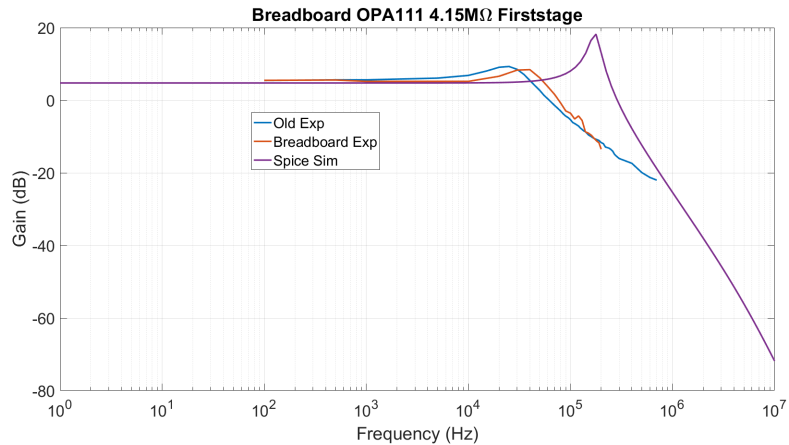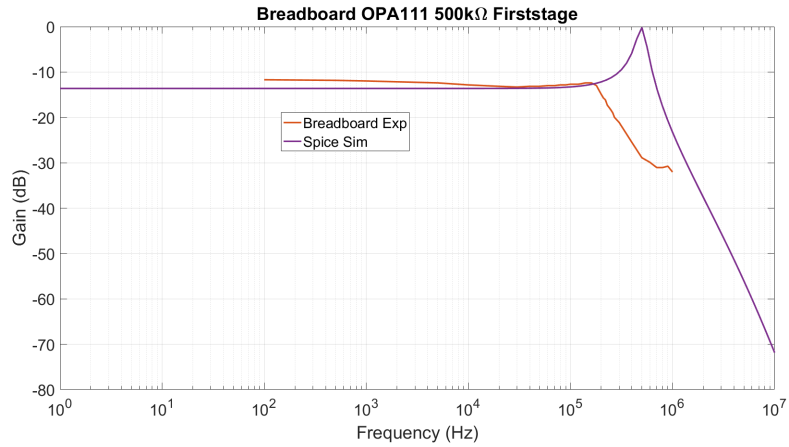
Figure 3.12:   Breadboard OPA111 500 kΩ. This plot shows gain for the first stage with the 500 kΩ feedback resistor of the breadboard simulation compared with the spice simulation for the circuit.

After comparing the breadboard simulation of OPA111 to the experimental and LTspice simulation data of the OPA111 preamp circuit, I switched the OPA111 op amp out for the OPA637 op amp and ran the same tests for both the 4.15 MΩ and the 500 kΩ feedback resistors in both the first stage alone as well as the combined stages. Unfortunately, the railing issue occurred for both the first and combined stages for the 4.15 MΩ resistor, so we were only were able to take data for the 500 kΩ resistor. We can see in Fig. 3.13 that this strange dip in the gain of the 500 kΩ feedback resister shows up with the OPA637 as well. The gain dips down until about 300 kHz rising up again at around 1 MHz. I even took the data multiple times to ensure that this was not an error. The high bandwidth is promising to our goal of 1 MHz, but the odd fluctuations in gain may give us an unstable signal when running the actual detector, which is not great for our experiments.
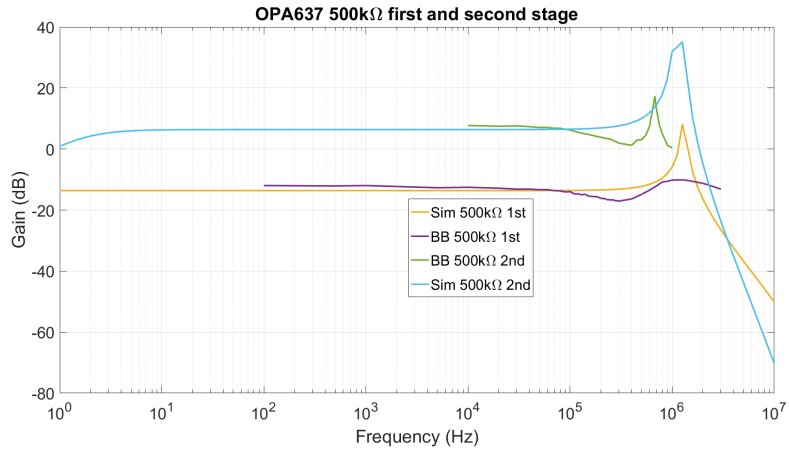
Figure 3.13: Breadboard OPA637. This plot shows the gain of the first and second stages of the breadboard circuit with the OPA637 op amp for the 500 kΩ feedback resistor in comparison to the spice simulation of the same circuit. BB and Sim stand for breadboard simulation, and spice simulation respectively.

I again switched out the op amps in the circuit for the THS4631 to take data for the breadboard circuit for both the 4.15 MΩ and 500 kΩ feedback resistors in both the first and combined stages. For the THS4631, we were able to take data for the 4.15 MΩ resistor for the first stage, but not the second stage. We can see in Fig. 3.14 that the breadboard simulation for the THS4631 circuit shows us a very similar story to that of the OPA637 circuit with 500 kΩ feedback resistor. The gain for the 4.15 MΩ feedback resistor seems to be more stable, but its bandwidth is much lower than that of the 500 kΩ feedback resistor.
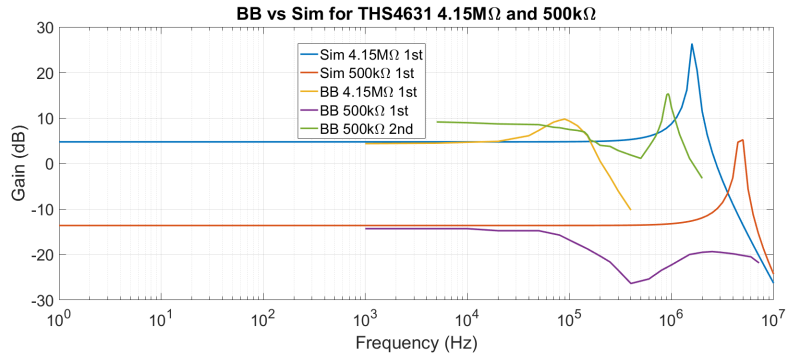
Figure 3.14: Breadboard THS4631. This plot shows the gain of the breadboard circuit for the THS4631 op amp in the first stage for the 4.15 MΩ and 500 kΩ feedback resistors as well as the combined stages for the 500 kΩ.

3.3.1 Adding Feedback Capacitor

From Op Amp Applications Handbook [9], I found that you can add a feedback capacitor in parallel to the feedback resistor to reduce oscillating noise that can occur with higher value feedback resistors. As seen from the parasitic capacitance tests done in the simulations where we varied the values of capacitance across different components, we noticed that the capacitance across the feedback resistor decreased the peak that occurred before the gain roll-off. This tells us that we could manually add a feedback capacitor to the OPA637 circuit as well as the THS4631 circuit to enable us to take data for the 4.15 MΩ feedback resistor. As the capacitance gets larger however, the bandwidth can suffer as we saw in Fig. 3.4. To test this, I first added a feedback capacitor of 1 pF across the feedback loop of the first stage and decreased the value each time to try and reach the highest bandwidth possible before the circuit begins to have the oscillating railing voltage issue that I mentioned earlier. For the OPA637 circuit, when testing the first stage alone, I was able to get a 0.25 pF feedback capacitor across the 4.15 MΩ feedback resistor, and this gave us a bandwidth of about 200 kHz, which is actually larger than the bandwidth of the THS4631 first

21

stage with the 4.15 MΩ resistor, which only gave us about 100 kHz. Unfortunately, when trying the first and second stage together for the OPA637 with the 4.15 MΩ resistor, I was unable to take data for a feedback capacitance lower than 1 pF; this gave us a bandwidth of about 40 kHz, which is nowhere near where we need it to be. This was the same for the THS4631 with the 4.15 MΩ feedback resistor with both stages connected, the lowest feedback capacitance achieved was 1 pF, and this gave us a bandwidth of abut 40 kHz. The issue here might be that the capacitance is not large enough to compensate for the oscillations coming from these larger feedback resistors.

3.4   Input Impedance

Since the resistance values we are dealing with are fairly high, 2.4 MΩ input resistor and 4.15 MΩ feedback resistor, I looked further into how these large values can affect the overall performance of the circuit. I tested this by switching out the 2.4 MΩ input resistor and 4.15 MΩ feedback resistor for a 200 kΩ input resistor and 402 kΩ feedback resistor. These resistors provide approximately the same gain to our amplifier, which means that the bandwidth should stay similar, but from Fig. 3.15, we see that this bandwidth actually increases for lower value resistors giving the same gain. We did not have the resistors on hand to test this for even lower values, but from the spice simulation of lower value resistors, we see that the trend continues.
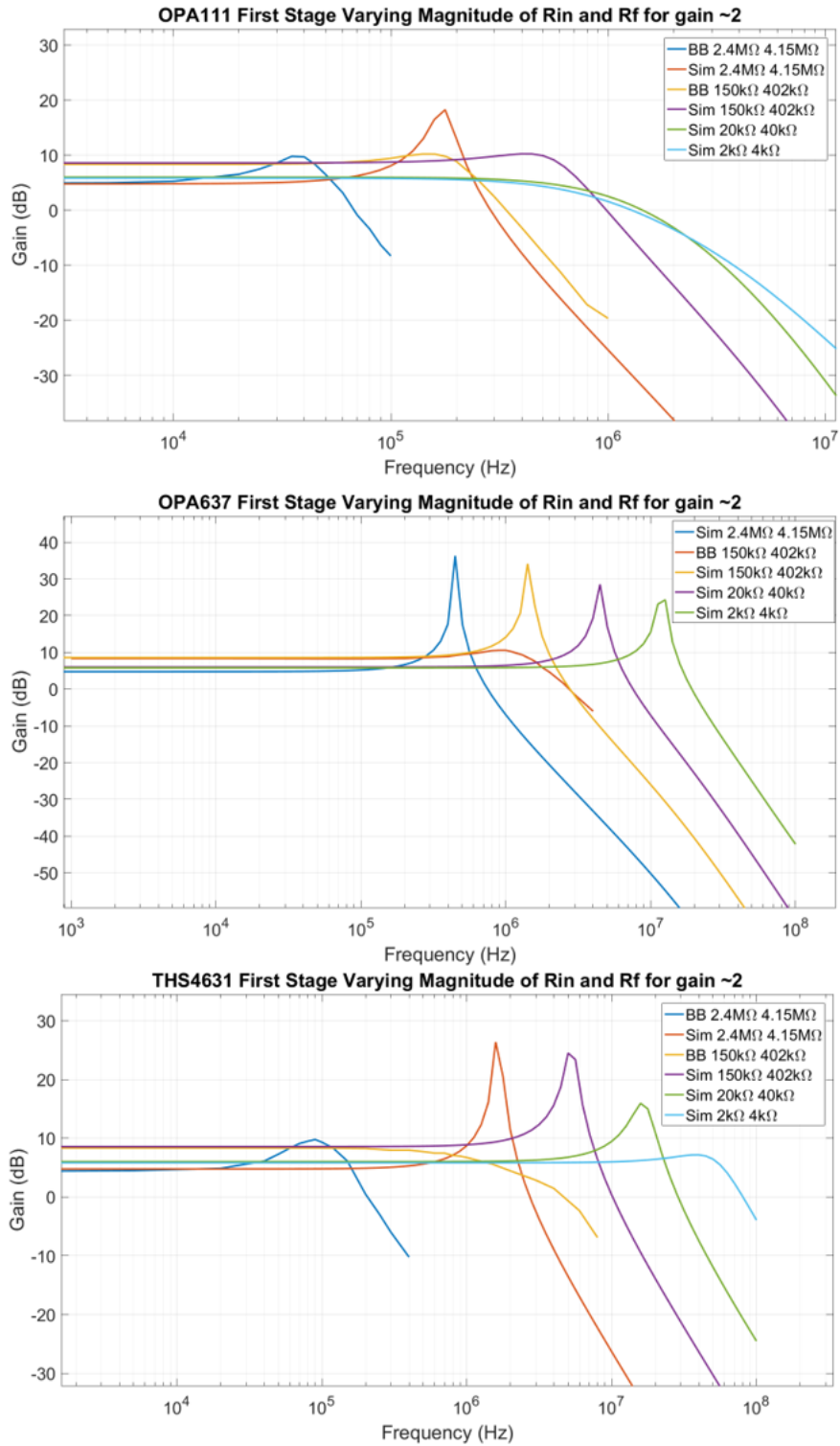
Figure 3.15: Varying Magnitude of Input and Feedback. This plot shows the frequency response of the OPA111-OPA27, OPA637-OPA637, and THS4631-THS4631 circuits for varying values of the input resistor and feedback resistor keeping the gain similar.

23

Looking into this, it turns out that at high enough resistance values for the input resistor, the input impedance of the op amp itself becomes comparable to a degree to the value of the input resistor itself. This causes the impedance of the op amp to act like a load, decreasing the overall gain of the circuit [12]. The rated input impedance for the THS4631 is $10^9\Omega$, which means that input resistance values in the MΩ range will begin to affect the performance of the circuit. However, the rated input impedance for the OPA111 and OPA637 op amps is $10^{13}\Omega$, so our input resistor of 2.4 MΩ should be affecting these op amps as much as we are noticing.

3.5 Increasing Second Stage Gain

Knowing that the THS4631 op amps are not going to be reliable for us with our higher input resistance values, I look closer into the OPA637 op amp and how to optimize our gain for this op amp. Since the 4.15 MΩ feedback resistor is severely limiting our gain, the 500 kΩ feedback resistor seems more promising, even with its much lower gain. One way to improve this low gain issue is to increase the gain in the second stage of the op amp. As mentioned earlier, the second stage is used purely to increase the gain of the signal coming from the first stage. To increase the gain for the second stage, you can either increase the value of the feedback resistor or lower the value of the input resistor. I chose to lower the input resistor by a factor of two by placing another 49.9 kΩ resistor in parallel with the existing one. This gives a gain of x20 in the second stage.

Unfortunately when I went to retake data of the OPA637 with the 500 kΩ feedback resistor in the first stage, the railing issue occurred here when it had not the previous times that I checked this configuration. I eventually solved this in a similar way that I solved the 4.15 MΩ resistor issue. Placing a 0.5 pF feedback capacitor across the 500 kΩ feedback capacitor allowed the circuit to work again, and this time, the overall

gain and bandwidth did not change very much from the data that I got before for the OPA637 with the 500 kΩ feedback resistor.

Increasing the gain in the second stage to x20 seemed to bring about the railing oscillations as well, so a 1 pF capacitor was needed to be placed across the 500 kΩ feedback resistor in the first stage to take data. In Fig. 3.16, you can see that the gain is in fact increased for the case of x20 in the second stage, as expected, however, the second peak that we were observing disappeared likely due to the fact that the feedback capacitance in the first stage was large enough to reduce the bandwidth past this point.
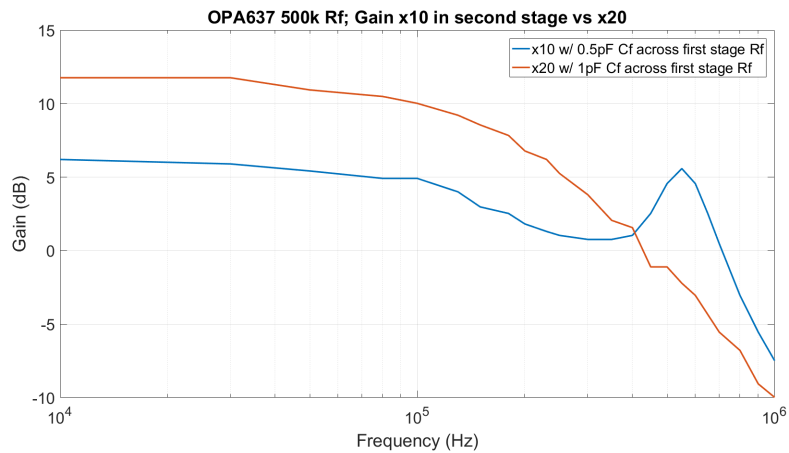
Figure 3.16: Increasing the gain in the second stage of OPA637 500 kΩ Rf. This plot shows the comparison of x10 gain vs x20 gain in the second stage of the circuit for OPA637 with the 500 kΩ feedback resistor.

3.6 Breadboard Parasitic Capacitance

Just as we accounted for the parasitic capacitance before using the spice simulation to see how the parasitic effects can change the circuit, it is important to measure these effects in our breadboard simulation of the circuit. We can measure capacitance on an oscilloscope by setting up an RC series circuit (where a resistor an capacitor are

in series) and sending a square wave input voltage through the circuit. Measuring the output voltage across the capacitor, we can calculate the time constant of the capacitor by measuring the point at which the capacitor has reached 63.2% of the total voltage. Normally, the capacitance can be calculated using the equation,

$$C = \frac{\tau}{R} \qquad (3.3)$$

where τ is the time constant and R is the value of the resistor [13]. For calculating the value of parasitic capacitance across a resistor, the equation changes slightly since now we must account for the resistor in parallel with the capacitor as well. This equation turns into

$$C = \frac{\tau(\frac{R_1}{R_2} + 1)}{R_1} \qquad , \qquad (3.4)$$

where R_1 is the same resistor as in the previous equation, and R_2 is the resistance of the resistor we are trying to calculate the capacitance of. As you can see, when the value of R_2 is much larger than the value of R_1, which is typical for most cases, this equation simplifies back down to Eq. 3.3.

Using the 50 Ω of input resistance from the function generator as R_1, I measured the time constant for both our 4.15 MΩ and 2.4 MΩ resistors because these were the resistors that would have the largest parasitic capacitances. I found a capacitance of 516 pF and 488 pF respectively, which is rather large compared to what our estimated values of parasitic capacitance for these resistors would be. Noticing that the time constant was reaching the limits of the oscilloscope (in the nanosecond range), I decided to increase the value of the input resistor to give a more accurate value of the time constant for the 4.15 MΩ and 2.4 MΩ resistors. for this, I used a 50 kΩ resistor, then again with a 500 kΩ resistor. From this, I found the values of capacitance of the 4.15 MΩ resistor to be 82.2 pF and then 58.3 pF. For the 2.4 MΩ resistor, I found 81.7 pF and 58 pF. These values are closer to what we estimated, but still large.

From our earlier simulations of the parasitic capacitance through Spice, we found that the parasitic capacitance that would most affect the overall bandwidth of our circuit is the stray capacitance from the wires going into the inverting input of the op amp to ground. In the breadboard simulation of this circuit however, we do not have these long wires that might be creating this capacitance. This stray capacitive effect can still occur on a breadboard between the rows that the op amp pins connect to. Because of the way that the rows of a breadboard are built, these parallel metal plates can cause a capacitance between each other, which at high frequencies, can be noticeable. We can measure this stray capacitance between breadboard rows in a very similar way, creating an effective RC series circuit and measuring the time constant from the output voltage across the two breadboard rows. Using the same values of resistance, 50 Ω, 50 kΩ, and 500 kΩ, I measured the time constant, and calculated the capacitance using Eq. 3.3. For these capacitances, I measured 492 pF, 87 pF, and 57.2 pF respectively. This means that the capacitance between the breadboard rows do have an impact on the bandwidth of our circuit.

Chapter 4

Discussion

From this data, we can see that the THS4631 op amp generally outperforms the OPA637 and OPA111 op amps, in terms of bandwidth, except in the case of the 4.15 MΩ for the first stage measurements where the OPA637 performs slightly better when we place a 0.25 pF feedback capacitor in parallel to the 4.15 MΩ feedback resistor. We also notice that the 500 kΩ feedback resistor always gives us a larger bandwidth than the 4.15 MΩ feedback resistor, as expected, but it also gives us more instability in the gain around the higher frequencies, as well as a much lower signal that we were already concerned about. With the unreliability of the THS4631, as well as it giving us a lower bandwidth for the 4.15 MΩ feedback resistor, I believe that the best choice currently would be to use the OPA637 op amp with the 500 kΩ feedback resistor. I choose this because the 4.15 MΩ feedback resistor does not seem to work very well when the two stages are connected and even though the gain drops slightly with the 500 kΩ feedback resistor, it still provides a decent bandwidth and works consistently with both of the stages connected. Increasing the gain in the second stage to x20 could also prove to be useful even if the overall bandwidth proves to be lower. This is because we have other AFM tips that oscillate at lower frequencies allowing us to access the 4$^{\text{th}}$ harmonic at around 200-400 kHz. If we were to use these tips, the higher gain should give better data, however, once we reach 350-400 kHz, the gain

x10 might be better since it is more consistent, and we would not need to worry about stability in gain as much.

Chapter 5

Conclusions and Outlook

With the information that I have acquired, I believe that the OPA637 op amp can provide us with the highest bandwidth for both the first and the second stages of the preamplifier circuit, based on experimental manipulations of the breadboard version of the same circuit. Since the OPA637 provides both a higher bandwidth for the 4.15 MΩ feedback resistor than the THS4631 and OPA111, and comparable bandwidth for the 500 kΩ feedback resistor to the THS4631, the best performing op amp that we have tested is the OPA637. The 500 kΩ resistor is also the best choice that we have for the feedback resistor. Even though the 4.15 MΩ has a higher and more consistent gain, the 500 kΩ resistor gives us a much better bandwidth, and has been able to perform when both stages are connected where the 4.15 MΩ feedback resistor has not. It remains to be seen how the preamp circuit of the detector will behave when we replace the OPA111 and OPA27 op amps with the faster OPA637 op amps.

Even though we can say that the OPA637 with the 500 kΩ feedback resistor gives us the largest bandwidth, we cannot be satisfied with the bandwidth being still under 1 MHz. It is possible to use different AFM tips which allow us to access the 4th harmonic at 200-400 kHz, but even with the OPA637 with a 500 kΩ feedback resistor, the gain is very low, giving us a smaller than desired signal in response when running the full detector for nanospectroscopy experiments. Increasing the gain to

x20 in the second stage gives us a better overall gain, however since there is a larger capacitance in the feedback of the first stage, the gain drops off with a larger slope, while the gain x10 stays slightly more stable. In the future, constructing this circuit on a printed circuit board (PCB) might give better and more conclusive results since a breadboard can produce even more parasitic capacitances and inductances apart from the ones that arise within the circuit itself. Because of this, a breadboard can sometimes cause problems for the circuit when operating at higher frequencies. A PCB would reduce these issues with much shorter and cleaner connections between components. The reason I chose to use a breadboard when experimenting with the circuits is because, as stated before, it provides a much easier and cheaper way of testing the circuit. A breadboard is also much easier to experiment on than a PCB, since you can constantly move components around and change the configuration of the circuit.

Bibliography

[1] Lipson, Lipson & Tannhauser (1998). "Optical Physics". United Kingdom: Cambridge.

[2] Hillenbrand, R. & Keilmann F. "Near-field microscopy by elastic light scattering from a tip: One contribution of 13 to a Theme 'Nano-optics and near-field microscopy'". Philosophical transactions. Series A, Mathematical, physical, and engineering sciences.

[3] Johnson, J.B.(1928). "Thermal Agitation of Electricity in Conductors". American Physical Society. Phys. Rev. vol.32.
`https://link.aps.org/doi/10.1103/PhysRev.32.97`

[4] Karki, J. (1998). "Understanding Operational Amplifier Speifications". Texas Intruments White Paper: SLOA011.
`http://www.ti.com/lit/an/sloa011/sloa011.pdf`

[5] Rogalski, A. (2011). "Infrared Detectors". 2nd ed. Boca Raton: CRC Press, Taylor and Francis.

[6] Woody, J.A. (1983). "Modeling of Parasitic Effects in Discrete Passive Components". Georgia Institue of Technology Final Technical Report.
`http://citeseerx.ist.psu.edu/viewdoc/download?doi=10.1.1.876.7842&rep=rep1&type=pdf`

[7] Jackson, J.D. (1962). "Classical Electrodynamics". 2nd ed. John Wiley & Sons.

[8] Grover, F. W. (1962). Inductance calculations. New York, NY: Dover.

[9] Jung, W. G. (2005). Op Amp applications handbook. Burlington, MA: Newnes.

[10] Horowitz, P., & Hill, W. (1989). The art of electronics (2nd ed.). Cambridge: Cambridge Univ. Press.

[11] Fink, D. G. (1975). Electronics Engineers' Handbook (1st ed.). McGraw-Hill.

[12] (2009). "Op Amp Input Impedance". Analog Devices: MT-040 `https://www.analog.com/media/en/training-seminars/tutorials/MT-040.pdf`

[13] Eggleston, D. L. (2011). Basic Electronics for scientists and engineers. Cambridge, UK: Cambridge University Press.

[14] Amenabar, I., Poly, S., Goikoetxea, M., Nuansing, W., Lasch, P., & Hillenbrand, R. (2017). Hyperspectral infrared nanoimaging of organic samples based on Fourier transform infrared nanospectroscopy. Nature Communications, 8, 14402. doi:10.1038/ncomms14402